# Waveform Distortions Due to Second-Order Dispersion and Dispersion Mismatches in a Temporal Pulse-Shaping System

Hao Chi and Jianping Yao, *Senior Member, IEEE, Member, OSA*

*Abstract*—Waveform distortions due to second-order dispersion (SOD) and dispersion mismatches in a temporal pulse-shaping (TPS) system for ultrashort arbitrary waveform generation (AWG) are studied in this paper. A closed-form analytical expression for the generated waveform incorporating the SOD and the dispersion mismatches is presented. A technique to eliminate the SOD-induced waveform distortions using a predistorted modulating signal is proposed. The influence of the limited bandwidth of the modulating signal on the waveform generation is studied. A comprehensive comparison between the TPS and the spatial-light-modulator-based techniques for AWG is also presented.

*Index Terms*—Arbitrary waveform generation (AWG), chromatic dispersion, fiber optics, Fourier transform, optical signal processing, temporal pulse shaping (TPS), ultrashort pulse.

## I. INTRODUCTION

SPATIAL-LIGHT-MODULATOR (SLM)-based pulse-shaping techniques have been intensively investigated for ultrafast arbitrary waveform generation (AWG), which has found many potential applications in high-speed communications, pulsed radar, instrumentation, and sensing [1]–[4]. In an SLM-based AWG system, a waveform synthesis is achieved by spatially masking the spatially dispersed spectrum of an ultrashort pulse, which is usually implemented using a pair of diffraction gratings and lenses. One of the major advantages of the SLM-based techniques is that the pattern on the SLM can be easily updated, leading to the generation of arbitrary waveforms in real time. However, a pulse-shaping system using an SLM involves fiber-to-space and space-to-fiber coupling, which makes the system bulky and complicated.

Recently, Azana *et al.* [5] proposed an approach based on temporal self-imaging for ultrafast AWG, with generated

H. Chi is with the Department of Information and Electronic Engineering, Zhejiang University, Hangzhou 310027, China, and also with the Microwave Photonics Research Laboratory, School of Information Technology and Engineering, University of Ottawa, Ottawa, ON K1N 6N5, Canada.

J. Yao is with the Microwave Photonics Research Laboratory, School of Information Technology and Engineering, University of Ottawa, Ottawa, ON K1N 6N5, Canada (e-mail: jpyao@site.uOttawa.ca).

waveforms having a frequency of up to hundreds of gigahertz. The temporal self-imaging phenomenon is utilized to realize frequency upshifting. This technique offers a feasible solution for the generation of ultrafast waveforms. However, there is an inherent constraint induced by the temporal Talbot effect, in which the microwave signal to be upshifted should be periodical or quasi-periodical such as a nonmodulated or slowly modulated microwave tone [6], [7].

AWG can also be implemented in the time domain using a temporal pulse-shaping (TPS) technique. A TPS system usually consists of two conjugate dispersive elements and an electrooptic modulator (EOM) that is placed between the two dispersive elements. In the TPS system, an ultrashort optical pulse is temporally stretched and spectrally dispersed by passing through the first dispersive element. Then, the dispersed pulse is spectrum-shaped in the time domain by modulating the spectrum with an RF signal at the EOM; the temporal compression is realized by passing the spectrum-shaped pulse through the second dispersive element. At the output of the system, a waveform that is the Fourier transform of the RF signal would be obtained. The concept of the TPS was originally proposed by Heritage and Weiner [8]. Recently, a comprehensive investigation of this technique was performed by Saperstein *et al.* [9], in which the modulating signal considered is a microwave tone, which would lead to the generation of two or three ultrashort pulses, depending on the bias voltage applied to the EOM. The application of the TPS technique in microwave spectrum analysis was reported in [10], where the temporal spacing between the generated short pulses is used to estimate the frequency of the RF modulating signal. If the EOM in the TPS system is a phase modulator, due to the modulating nonlinearity of the phase modulator, more ultrashort pulses with a controllable repetition rate could be generated [11].

The TPS is an attractive technique for AWG since it is realized in a fiber-optic platform without the requirement of any bulky optical devices. As we know, the highest frequency of an arbitrary waveform using an electrical arbitrary waveform generator is limited to around 10 GHz. By using the TPS technique, an arbitrary waveform with a much higher frequency can be generated using a low-frequency electrical waveform from a currently available electrical arbitrary waveform generator. In addition, as we have demonstrated recently, a symmetrical waveform can be generated using an amplitude-only modulator in a TPS system [12], which makes the system greatly simplified compared to an SLM-based system,

Fig. 1. Schematic diagram of the TPS system for arbitrary waveform generation (FSPL: Femtosecond pulse laser; EOM: Electrooptic modulator; DAC: Digital-to-analog converter).

in which both the amplitude and the phase should be encoded, even for a real modulating signal with both positive and negative values, which requires an amplitude modulator and a phase modulator.

In this paper, we study some important issues of the TPS technique for practical applications. In an ideal TPS system, the two conjugate dispersive elements should be perfectly matched in the first-order dispersion (FOD) and free of second-order dispersion (SOD). In a real system, however, the existence of a SOD and dispersion mismatches is inevitable, which would lead to the distortions of the generated waveforms. In this paper, we present, for the first time, to the best of our knowledge, a comprehensive investigation on the effects of the SOD and the dispersion mismatches that would lead to distortions to the generated ultrafast waveforms. A closed-form analytical expression for the generated waveform in a TPS system that incorporates the SOD and the dispersion mismatches is presented, where the modulating input to the EOM could be any signal (not limited to a microwave tone). The effects of the SOD and dispersion mismatches that lead to distortions to the generated waveform can be readily estimated according to the derived analytical expressions. To eliminate the SOD-induced waveform distortion, a predistortion technique is proposed. In addition, the influence of the limited bandwidth of the modulating signal on the waveform generation is studied. Finally, a comprehensive comparison between the TPS and the SLM-based techniques is presented.

## II. THEORETICAL MODEL

The schematic diagram of a TPS system for AWG is shown in Fig. 1. The system consists of a femtosecond pulsed laser (FSPL), two conjugate dispersive elements, and an EOM that is placed between the two dispersive elements. A pattern generator is used to generate a low-frequency electrical waveform. For generality, both the FOD $\ddot{\Phi}$ and the SOD $\dddot{\Phi}$ are taken into account in the analysis. The FOD $\ddot{\Phi}$ and the SOD $\dddot{\Phi}$ are given by $\ddot{\Phi} = \ddot{\beta}z$ and $\dddot{\Phi} = \dddot{\beta}z$, where $z$ is the length of dispersive element, and $\ddot{\beta}$ and $\dddot{\beta}$ denote, respectively, the second-order and the third-order derivatives of the propagation constant $\beta$ with respect to the angular frequency $\omega$. The dispersion mismatches between the two dispersive elements $\delta\ddot{\Phi}$ and $\delta\dddot{\Phi}$ are also considered. In the following analysis, for simplicity, we ignore the average group delay introduced by the dispersive elements.

Assume that the input optical pulse $g(t)$ is a transform-limited ultrashort Gaussian pulse, which is expressed as

$$g(t) = \exp\left(-\frac{t^2}{\tau_0^2}\right) \tag{1}$$

where $2\tau_0$ is the full width at $1/e$ of maximum. Its Fourier transform[1] is given by

$$\widetilde{G}(\omega) = \Im\{g(t)\} = \sqrt{\pi}\tau_0 \exp\left(-\frac{\tau_0^2\omega^2}{4}\right). \tag{2}$$

The transfer functions of the first and the second dispersive elements are, respectively, given by

$$H_{\ddot{\Phi}+\dddot{\Phi}} = \exp\left[-j\left(\frac{\ddot{\Phi}\omega^2}{2} + \frac{\dddot{\Phi}\omega^3}{6}\right)\right] \tag{3}$$

and

$$H_{-\ddot{\Phi}-\dddot{\Phi}} = \exp\left[j\left(\frac{\ddot{\Phi}\omega^2}{2} + \frac{\dddot{\Phi}\omega^3}{6}\right)\right]. \tag{4}$$

If a modulating signal $x(t)$ is applied to the EOM, the Fourier transform of the signal at the output of the EOM is given by

$$\widetilde{Q}(\omega) = \frac{1}{2\pi}\left[\widetilde{G}(\omega)H_{\ddot{\Phi}+\dddot{\Phi}}\right] * \widetilde{X}(\omega) \tag{5}$$

where $\widetilde{X}(\omega)$ is the Fourier transform of $x(t)$, and $*$ denotes the convolution operation. Here, a linear modulation is assumed.

Substituting the expressions of $\widetilde{G}(\omega)$ in (2) and $H_{\ddot{\Phi}+\dddot{\Phi}}$ in (3) into (5), we have

$$\widetilde{Q}(\omega) = \frac{1}{2\pi}\int_{-\infty}^{\infty}\widetilde{X}(\Omega)\widetilde{G}(\omega-\Omega)H_{\ddot{\Phi}+\dddot{\Phi}}(\omega-\Omega)d\Omega$$

$$= \frac{1}{2\pi}\sqrt{\pi}\tau_0\exp\left(-\frac{\tau_0^2\omega^2}{4}\right)\exp\left(-j\frac{\ddot{\Phi}\omega^2}{2}\right)\exp\left(-j\frac{\dddot{\Phi}\omega^3}{6}\right)$$

$$\times \int_{-\infty}^{\infty}\widetilde{X}(\Omega)\exp\left[\left(-j\ddot{\Phi}+\frac{\tau_0^2}{2}\right)\left(\frac{\Omega^2}{2}-\omega\Omega\right)\right]$$

$$\times \exp\left[-j\dddot{\Phi}\left(\frac{-3\omega^2\Omega+3\omega\Omega^2-\Omega^3}{6}\right)\right]d\Omega \tag{6}$$

where $\Omega$ is the integration variable. If the width of the input pulse $\tau_0$ is sufficiently small and the FOD $\ddot{\Phi}$ is sufficiently large such that

$$\left|\frac{\tau_0^2}{\ddot{\Phi}}\right| \ll 1 \tag{7}$$

---

[1]Here, we use the definition of the Fourier transform as $\widetilde{G}(\omega) = \int_{-\infty}^{\infty}g(t)\exp(-j\omega t)dt$.

and the spectrum of $x(t)$ is confined to a narrow region $\Delta\omega_m$ such that

$$\tau_0 \Delta\omega_m \ll 1 \tag{8}$$

by employing a similar treatment as in [13] and [14], the exponential term in the integral in (6) can be approximated as $\exp[j\Omega(\ddot{\Phi}\omega + \dddot{\Phi}\,\omega^2/2)]$ by ignoring the terms $\tau_0^2$, $\Omega^2$, and $\Omega^3$. Thus, $\widetilde{Q}(\omega)$ can be rewritten as

$$\widetilde{Q}(\omega) \cong \widetilde{G}(\omega)\exp\left(-j\frac{\ddot{\Phi}\omega^2}{2}\right)\exp\left(-j\frac{\dddot{\Phi}\omega^3}{6}\right)$$
$$\times \Im^{-1}\left\{\widetilde{X}(\omega)\right\}\big|_{t=\ddot{\Phi}\omega+\dddot{\Phi}\omega^2/2} \tag{9}$$

where $\Im^{-1}\{\cdot\}$ denotes the inverse Fourier transform, and we have $\Im^{-1}\{\widetilde{X}(\omega)\}\big|_{t=\ddot{\Phi}\omega+\dddot{\Phi}\omega^2/2} = x(\ddot{\Phi}\omega + \dddot{\Phi}\omega^2/2)$.

We have used conditions in (7) and (8) to approximate (6) by (9), which imposes constraints on the temporal width $\tau_0$ of the input pulse $g(t)$, the FOD coefficient $\dddot{\Phi}$, and the bandwidth $\Delta\omega_m$ of the modulating signal $x(t)$. It is worth noting that (7) and (8) are sufficient, but maybe not necessary, conditions to approximate (6) by (9). Exact conditions for temporal spectral shaping without higher order dispersion were derived in [15] by Azana, which imposes looser constraints on $\tau_0$, $\ddot{\Phi}$, and $\Delta\omega_m$.

Therefore, if the dispersion mismatches are ignored, the spectrum of the output signal can be expressed as

$$\widetilde{Y}(\omega) = \widetilde{Q}(\omega)H_{-\ddot{\Phi}-\dddot{\Phi}} = \widetilde{G}(\omega)x\left(\ddot{\Phi}\omega + \frac{\dddot{\Phi}\omega^2}{2}\right) \tag{10}$$

and the corresponding temporal signal is given by

$$y(t) = \Im^{-1}\{Y(\omega)\} = g(t) * \Im^{-1}\left\{x\left(\ddot{\Phi}\omega + \frac{\dddot{\Phi}\omega^2}{2}\right)\right\}. \tag{11}$$

In a TPS system with only FOD ($\dddot{\Phi} = 0$), we have

$$y(t) = \frac{1}{|\ddot{\Phi}|}g(t) * \widetilde{X}\left(\frac{t}{\ddot{\Phi}}\right). \tag{12}$$

It is simply a convolution of a scaled version of the Fourier transform of $x(t)$ with the input ultrashort pulse $g(t)$.

In general, $x(t)$ should be a complex signal for AWG, which would be implemented using both an amplitude modulator and a phase modulator. The use of an amplitude modulator and a phase modulator makes the system very complicated; in particular, a precise synchronization between the amplitude signal and the phase signal must be ensured. For many applications, however, the waveforms are inherently symmetrical, such as a square wave, a triangular wave, or a doublet. It is known that, for a real and symmetrical signal, its Fourier transform is also real and symmetrical. It is therefore possible to generate a symmetrical waveform with a real and symmetrical modulating signal using only an amplitude modulator [12]. For example,

we can bias a Mach–Zehnder modulator at the minimum transmission point, with a modulating signal that is real with both positive and negative values.

In (11), we can see that the output waveform would be distorted if $\dddot{\Phi}$ is not zero. In order to eliminate the SOD-induced waveform distortion, we propose a predistortion technique in which a predistorted modulating signal is used. Based on (10), a predistorted signal $x'(t)$ is constructed to satisfy

$$x'\left(\ddot{\Phi}\omega + \frac{\dddot{\Phi}\omega^2}{2}\right) = x(\ddot{\Phi}\omega) \tag{13}$$

where the inverse Fourier transform of $x(\ddot{\Phi}\omega)$, $\widetilde{X}(t/\ddot{\Phi})$ is the required output waveform. According to (13), $x'(t)$ can be obtained by variable substitution

$$x'(t) = x\left(\frac{-1 + \sqrt{1 + 2t\dddot{\Phi}/\ddot{\Phi}^2}}{\dddot{\Phi}/\ddot{\Phi}^2}\right)$$
$$\begin{cases} t \geq -\ddot{\Phi}^2/(2\dddot{\Phi}), & \text{if } \dddot{\Phi} > 0 \\ t \leq -\ddot{\Phi}^2/(2\dddot{\Phi}), & \text{if } \dddot{\Phi} < 0 \end{cases}. \tag{14}$$

It is shown that the predistorted signal $x'(t)$ is a truncated signal. To achieve good performance using predistortion, according to (14), it requires that the original signal $x(t)$ is time-limited or its major part is confined to $t \geq -\ddot{\Phi}^2/\dddot{\Phi}$ (if $\dddot{\Phi} > 0$) or $t \leq -\ddot{\Phi}^2/\dddot{\Phi}$ (if $\dddot{\Phi} < 0$).

Now, we consider the influence of the dispersion mismatches. For simplicity, we assume that the SOD-induced waveform distortions are fully compensated by the proposed predistortion technique. Therefore, the spectrum of the output waveform with the dispersion mismatches $\delta\ddot{\Phi}$ and $\delta\dddot{\Phi}$ can be expressed as

$$\widetilde{Y}(\omega) = \widetilde{G}(\omega)x(\ddot{\Phi}\omega) \cdot \exp\left[-j\left(\frac{\delta\ddot{\Phi}\omega^2}{2} + \frac{\delta\dddot{\Phi}\omega^3}{6}\right)\right] \tag{15}$$

where $\exp[-j(\delta\ddot{\Phi}\omega^2/2 + \delta\dddot{\Phi}\omega^3/6]$ is the transfer function of the mismatched dispersion $\delta\ddot{\Phi}$ and $\delta\dddot{\Phi}$. In this case, the output temporal waveform can be expressed as

$$y(t) = \Im^{-1}\left\{\widetilde{Y}(\omega)\right\} = \frac{1}{|\ddot{\Phi}|}r(t) * \widetilde{X}\left(\frac{t}{\ddot{\Phi}}\right) \tag{16}$$

where $r(t)$ denotes an output pulse when the input is the Gaussian pulse $g(t)$ that has experienced the mismatched dispersion $\delta\ddot{\Phi}$ and $\delta\dddot{\Phi}$. $r(t)$ can be analytically expressed using the Airy function. The width of $r(t)$ is larger than that of the original pulse $g(t)$, which would degrade the waveform generated. The detailed property of $r(t)$ can be found in [16] and [17].

It is interesting to discuss the reference value of the dispersion mismatches that can be tolerated in the TPS system.

According to (15), the influence of the mismatched dispersion $\delta\ddot{\Phi}$ and $\delta\dddot{\Phi}$ could be negligible if the following inequality is satisfied:

$$\frac{1}{2}\delta\ddot{\Phi}\Delta\omega_p^2 + \frac{1}{6}\delta\dddot{\Phi}\,\Delta\omega_p^3 \ll 2\pi \tag{17}$$

where $\Delta\omega_p$ is the bandwidth of the input short pulse $g(t)$ [i.e., the operation optical bandwidth decided by $\widetilde{G}(\omega)$]. According to (17), we can set an upper limit on the dispersion mismatches that can be tolerated as $\delta\ddot{\Phi}\Delta\omega_p^2/2 + \delta\dddot{\Phi}\,\Delta\omega_p^3/6 = 2\pi\xi$, where $\xi$ is a small value, such as $1/100$ or $1/200$, which depends on the acceptable waveform distortion for practical applications.

By now, a general analysis on the TPS system that has the SOD and the dispersion mismatches has been presented. In the theoretical treatment, two approximation conditions in (7) and (8) are considered. The first inequality in (7) is the well-known time-domain Fraunhofer condition that imposes a lower limit on the FOD in the system, whereas the second inequality in (8) imposes a limit on the highest frequency of the modulating signal applied to the EOM, both for a given initial pulsewidth. It is worth noting that, for practical applications, these two conditions can be easily satisfied, which is verified by the following numerical results.

## III. RESULTS

To verify the theoretical analysis, numerical simulations are implemented. In the simulations, we assume that the input optical pulse has a Gaussian envelope with a full-width at half-maximum of 350 fs. The generation of a picosecond rectangular pulse is simulated. Since the rectangular wave is a symmetrical waveform, it can be realized using only an amplitude modulator, as discussed above. In the simulation, the FOD $\ddot{\Phi}$ is set at 1000 ps², which is approximately equal to the accumulated dispersion of a 50-km standard single-mode fiber. The value of $|\tau_0^2/\ddot{\Phi}|$ is calculated to be around $10^{-4}$; thus, the first approximation condition in (7) is well satisfied. To account for the limited sampling rate of a digital-to-analog converter (DAC) in the pattern generator, the maximum frequency of the input modulating signal is set to be less than 1 GHz, which corresponds to a maximum sampling rate of 2 Gs/s.

It should be noted that, for carrier suppression, the EOM in the TPS system is biased at the minimum transmission point. Fig. 2 shows the schematic diagram of the modulation process for an input RF waveform with the EOM biased at different bias points. In a conventional subcarrier transmission system where intensity modulation with direct detection is considered, a bias at $V_\pi$ means a frequency doubling. However, in the TPS system, since we are concerned with the electrical field instead of the intensity, a bias at $V_\pi$ means a linear operation with carrier suppression.

### A. Ideal Case (Without SOD, Perfect FOD Match)

First, we study an ideal case in which the SOD is zero and the FOD is perfectly matched, i.e., $\dddot{\Phi} = 0$ and $\delta\ddot{\Phi} = \delta\dddot{\Phi} = 0$.
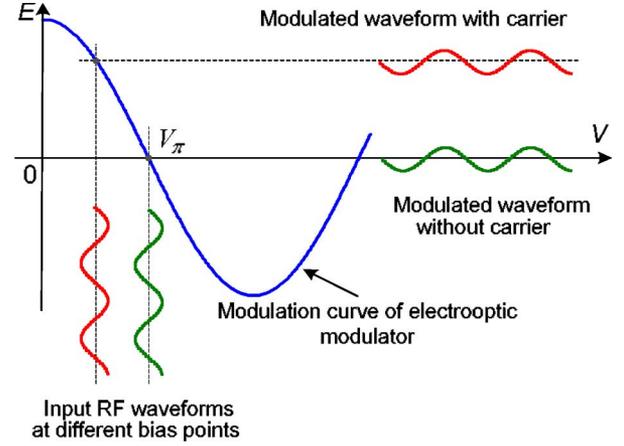


Fig. 2. Schematic diagram of the modulation process for an input RF waveform with the EOM biased at different points.
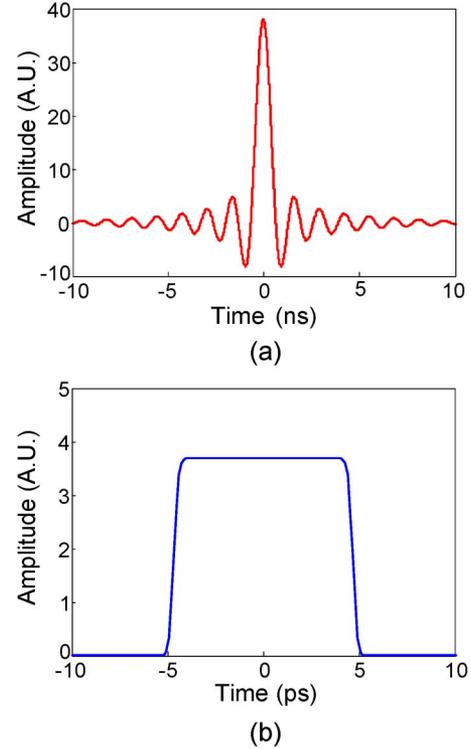


Fig. 3. Ideal case with perfect dispersion match and without SOD ($\ddot{\Phi} = 1000$ ps², $\dddot{\Phi} = 0$, and $\delta\ddot{\Phi} = \delta\dddot{\Phi} = 0$). (a) Sinc function applied to the EOM. (b) Generated square waveform.

It is known that the Fourier transform of a square wave is a sinc function. Therefore, a sinc function is applied to the EOM, as shown in Fig. 3(a). The value of $\tau_0\omega_m$ is calculated to be around $10^{-4}$; thus, the second approximation condition in (8) is also well satisfied. The system output is a convolution of a rectangular wave with the input ultrashort pulse, as shown in Fig. 3(b). The output pulsewidth is much narrower than that of the input modulating signal. Therefore, a high-frequency waveform can be generated using a low-frequency modulating signal in the TPS system. Note that the modulating signal is a bandwidth-limited signal, with a maximum frequency of around 0.80 GHz, which could be generated using a DAC with
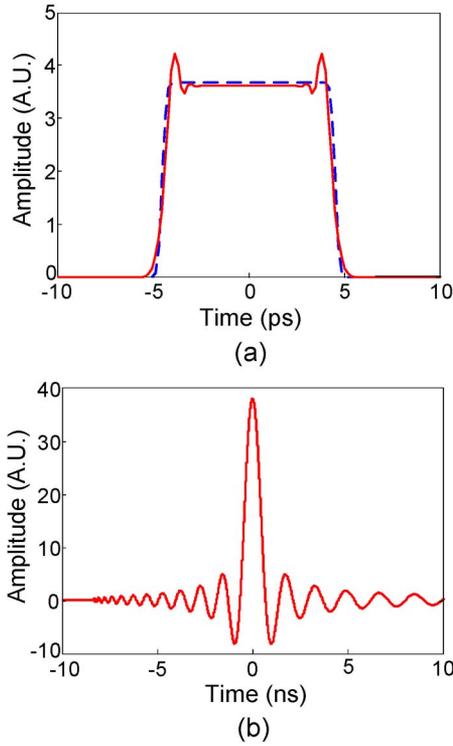
Fig. 4. Case with perfect dispersion match in FOD and SOD. (a) Generated waveform for $\ddot{\Phi} = 1000$ ps$^2$, $\dddot{\Phi} = 60$ ps$^3$, and $\delta\ddot{\Phi} = \delta\dddot{\Phi} = 0$. Solid curve: Without predistortion. Dashed curve: With predistortion. (b) Predistorted modulating signal when $\ddot{\Phi} = 1000$ ps$^2$ and $\dddot{\Phi} = 60$ ps$^3$.

a maximum sampling rate of about 2 Gs/s. We can also generate the same waveform using a modulating signal with a lower frequency, but a larger $\ddot{\Phi}$ is required, as indicated in (12).

### B. Case With SOD, Perfect Match

Then, we study the case in which a SOD is considered while keeping a perfect match in the FOD and the SOD (i.e., $\dddot{\Phi} \neq 0$ and $\delta\ddot{\Phi} = \delta\dddot{\Phi} = 0$). In the simulation, the FOD is still set at 1000 ps$^2$, and the SOD $\dddot{\Phi}$ is chosen to be 60 ps$^3$. Although, for a standard single-mode fiber with a FOD of 1000 ps$^2$, the SOD is 4–6 ps$^3$, the SOD can be much greater for other types of fiber. In addition, the SOD-induced waveform distortion would be shown more clearly when we set a larger SOD in the numerical simulation.

The generated distorted waveform is shown as the solid curve in Fig. 4(a). To eliminate the SOD-induced waveform distortion, a predistorted signal calculated based on (14), as shown in Fig. 4(b), is used to replace the original sinc function. In this case, the generated waveform, which is shown by the dashed curve in Fig. 4(b), is the same as the previously generated waveform in Fig. 3(b). Therefore, the effectiveness of the predistortion technique is verified.

### C. Case With Dispersion Mismatch

In a practical system, a perfect match in dispersions is very difficult to realize. Therefore, the influence of the dispersion
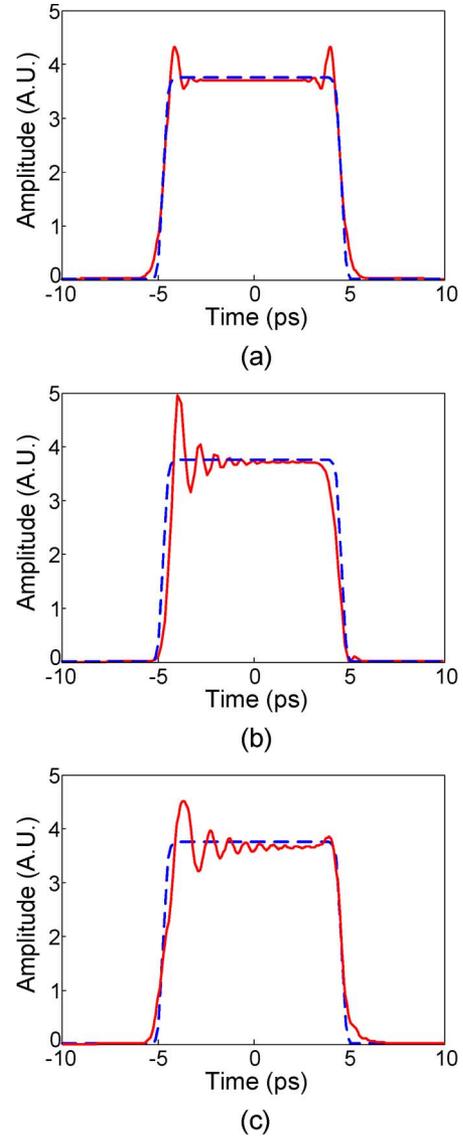


Fig. 5. Case with dispersion mismatch. (a) Generated waveform: $\ddot{\Phi} = 1000$ ps$^2$, $\dddot{\Phi} = 60$ ps$^3$, $\delta\ddot{\Phi} = 0.15$ ps$^2$, $\delta\dddot{\Phi} = 0$, with predistortion. (b) Generated waveform: $\ddot{\Phi} = 1000$ ps$^2$, $\dddot{\Phi} = 60$ ps$^3$, $\delta\ddot{\Phi} = 0$, $\delta\dddot{\Phi} = 0.08$ ps$^3$, with predistortion. (c) Generated waveform: $\ddot{\Phi} = 1000$ ps$^2$, $\dddot{\Phi} = 60$ ps$^3$, $\delta\ddot{\Phi} = 0.15$ ps$^2$, $\delta\dddot{\Phi} = 0.08$ ps$^3$, with predistortion.

mismatches in $\ddot{\Phi}$ and $\dddot{\Phi}$ on the generated waveform should be taken into account in the system design. Fig. 5(a) shows the case with a perfect match in $\ddot{\Phi}$ but a mismatch in $\ddot{\Phi}$ ($\delta\ddot{\Phi} = 0.15$ ps$^2$ and $\delta\dddot{\Phi} = 0$), where the predistortion technique is applied (which eliminates the effect of $\dddot{\Phi}$ despite of the fact that we still set $\dddot{\Phi}$ at 60 ps$^3$). It is interesting to find that the effect of the mismatch in $\ddot{\Phi}$ ($\delta\ddot{\Phi} \neq 0$) on the generated waveform is similar to the effect resulting from the nonzero $\dddot{\Phi}$ [as shown in Fig. 4(a)].

We then simulate the case of a perfect match in the FOD but a mismatch in the SOD (i.e., $\dddot{\Phi} \neq 0$, $\delta\ddot{\Phi} = 0$, and $\delta\dddot{\Phi} \neq 0$. The result is shown in Fig. 5(b), where $\delta\dddot{\Phi}$ is set at 0.08 ps$^3$. Compared with the SOD-induced waveform distortions,

the effect of the SOD mismatch is much more severe. Fig. 5(c) shows the case of mismatches both in $\ddot{\Phi}$ and $\dddot{\Phi}$ ($\delta\ddot{\Phi} = 0.15$ ps$^2$, and $\delta\dddot{\Phi} = 0.08$ ps$^3$). For comparison, the waveform generated in the case of a perfect dispersion match is shown here as the dashed waveform. Note that $\delta\ddot{\Phi} = 0.15$ ps$^2$ is approximately equal to the accumulated dispersion of only an 8-m-long standard single-mode fiber.

In addition, to verify the derived theoretical expressions, we also calculate all waveforms in Figs. 3–5 according to (11) and (16); the results exactly match those by simulations.

## IV. DISCUSSIONS

### A. Limited Sampling Rate of the DAC on the Waveform Generation

According to (12), the temporal width $T$ of the generated waveform is proportional to the bandwidth $B$ of the modulating signal $x(t)$ as $T = 2\pi|\ddot{\Phi}|B$. Therefore, the maximum temporal width of the generated waveform is limited by the bandwidth of $x(t)$. In the given example ($\ddot{\Phi} = 1000$ ps$^2$, $B = 2$ GHz), the maximum temporal width that can be achieved is around 12.6 ps. To achieve wider waveform, a larger FOD is required.

We have demonstrated the effectiveness of the proposed predistortion technique. However, the predistorted modulating signal shown in Fig. 4(b) is not a bandwidth-limited signal, which could not be realized by using a DAC with a limited sampling rate. Assuming that the sampling rate of the DAC is 2 Gs/s, the signal shown in Fig. 4(b) is then applied to a low-pass filter with a maximum frequency of 1 GHz. The bandwidth-limited predistorted signal and the generated waveform are shown in Fig. 6(a) and (b), respectively. It is found that the generated waveform is slightly distorted due to the limited bandwidth of the modulating signal, but it is much less distorted compared to the generated waveform without predistortion.

### B. Dispersion Mismatch and Compensation

Standard single-mode fiber and dispersion compensating fiber could be used as the dispersive elements with a perfect FOD match, but it is difficult to match the SOD at the same time. It is found that the SOD-induced waveform degradation could be well compensated by the proposed predistortion technique. Therefore, the effect of the dispersion mismatches, particularly the SOD mismatch, becomes a major source that deteriorates the waveform generation. A possible solution is to use a specially designed chirped fiber Bragg grating (CFBG), in which the FOD and SOD can be controlled separately [18]. Active dispersion compensation techniques based on phase modulation can also be considered to suppress the waveform distortion induced by the residual higher order dispersion [19], [20].

### C. Influence of Polarization-Mode Dispersion (PMD)

In a TPS system that uses fiber as dispersive element, PMD may not be negligible. From the results in Section III-C, we can see that the dispersion mismatch that resulted from
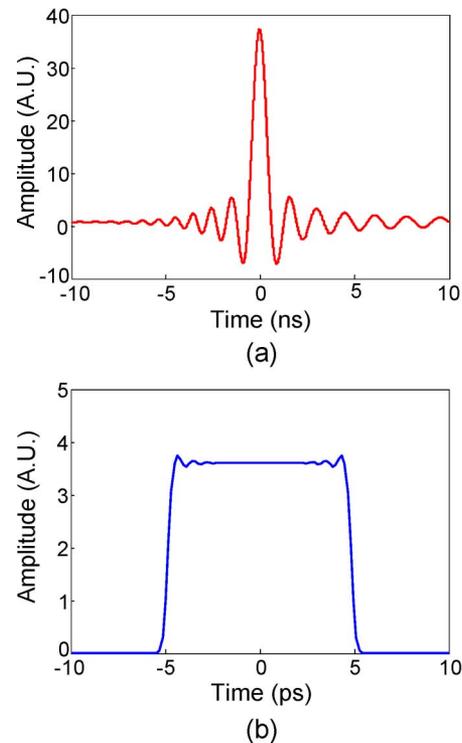


Fig. 6. Effects of the limited DAC sampling rate on the waveform generation. (a) Bandwidth-limited predistorted modulating signal. (b) Generated waveform.

several meters of fiber would lead to considerable waveform distortion. Based on the parameters given in Section III, a dispersion of 1000 ps$^2$ is applied in the TPS system, which is roughly equivalent to the accumulated dispersion of a 50-km standard single-mode fiber. According to the typical PMD value $\leq 0.1$ ps/$\sqrt{\text{km}}$ in the standard single-mode fiber, the accumulated differential group delay (DGD) in the total TPS system is around $\leq 1$ ps, which is nearly on the order of the width of the generated rectangular wave ($\sim$10 ps). A detailed analysis on this issue is out of the scope of this paper. From the point of view of the PMD-induced waveform distortion, optical fiber may not be the best candidate to serve as the dispersive elements applied in the TPS system. Due to the low-dispersion nature of the conventional fiber, typically, at least, tens of kilometers of fiber should be used in the system, which would lead to considerable DGD that would deteriorate the generated waveform. This problem can be overcome by using CFBGs with a large dispersion as the dispersive elements in the TPS system due to the shorter length required and, therefore, the low accumulated DGD induced by the CFBGs.

### D. Asymmetrical Waveform Generation

We have demonstrated that a symmetrical waveform could be generated using an amplitude-only modulator. For the generation of an asymmetrical waveform, both an amplitude modulator and a phase modulator are required. In this case, the amplitude signal and the phase signal should be synchronized accurately.

*E. Comparison Between the TPS and the SLM-Based Techniques*

The TPS technique is implemented in an optical fiber-based platform. Compared with an SLM-based AWG system, the TPS technique features a smaller size and a better stability. In addition, the use of fiber-optic components has the potential for integration using photonic integrated-circuit techniques.

In both approaches, a dispersion-free operation is required, i.e., in the absence of an SLM or a temporal optical modulator, the output pulse should be identical to the input pulse. In an SLM-based system, this can be guaranteed if the lenses are set up as a unit magnification telescope, with the gratings located outside the focal planes of the telescope [1]. In our approach, if the standard single-mode fiber and dispersion compensating fiber are used, a higher order dispersion mismatch would occur, which leads to pulse broadening in the absence of the modulation, with a degraded temporal resolution of the generated waveforms. Therefore, a careful control of the dispersion in the TPS technique is required.

One of the major advantages of the TPS technique is the generation of arbitrary symmetrical waveforms without the need of a phase modulator. In an SLM-based approach, however, to generate waveforms such as rectangular wave, both an amplitude modulator and a phase modulator are required [1]. Although the use of phase-only modulation can also generate a large variety of waveforms in the SLM-based system, there is no direct analytical solution to derive a phase-shift function that can approximate the desired output waveform. One of the available solutions is to use a time-consuming optimization algorithm, such as genetic algorithm or simulated annealing [21], [22].

In an SLM-based system, the use of a programmable SLM, either operating in phase only or in both phase and amplitude, would enable the generation of arbitrary waveforms in real time. In a TPS system, a low-frequency electrical signal is used to generate a high-speed signal. In other words, the TPS technique enables the generation of high-speed arbitrary waveforms that could not be directly generated in the electrical domain using an all-electrical arbitrary waveform generator.

In an SLM-based system, the finite aperture of the lens would limit the achievable temporal resolution of the system. In a TPS system, the temporal aperture is limited by the pulse interval of the applied mode-locked fiber laser (MLFL). A high repetition rate means a small temporal aperture in the TPS system. However, for a typical MLFL with a repetition rate at tens of megahertz (equivalent to $\sim$100-ns pulse interval), its influence on the temporal resolution is negligible.

In an SLM-based system, the pixelation of a programmable SLM, which corresponds to spectral sampling, would produce a staircase approximation of the desired waveform [1]. In a TPS system, the finite-bit resolution of the DAC in the applied pattern generator would give rise to the similar effect.

In addition, in a TPS system using optical fiber as dispersive elements, PMD in fiber must be taken into account in the system design. However, SLM-based systems are usually not affected by PMD.

Finally, in an SLM-based system, a good alignment between the input pulse and the pattern on the SLM is required. In a TPS system, instead of an accurate spatial alignment, a strict synchronization between the modulating signal and the input short pulse in time is required.

## V. CONCLUSION

In conclusion, a comprehensive study on the TPS system for AWG was presented. A closed-form analytical expression for the generated waveform in a TPS system incorporating the SOD and the dispersion mismatches was derived, which was verified by numerical simulations. With the given theoretical results, it is convenient to evaluate and predict the performance of a TPS system that has the SOD and the dispersion mismatches. A pre-distortion technique to eliminate the SOD-induced waveform distortion was proposed, which was also verified by numerical simulations. We also discussed the influence of the limited bandwidth of the modulating signal on waveform generation. Compared with the SLM-based AWG technique, the TPS technique can be implemented using fiber-optic components, which offers a potential for integration.

## REFERENCES

[1] A. M. Weiner, "Femtosecond pulse shaping using spatial light modulators," *Rev. Sci. Instrum.*, vol. 71, no. 5, pp. 1929–1960, May 2000.

[2] J. D. McKinney, D. E. Leaird, and A. M. Weiner, "Millimeter-wave arbitrary waveform generation with a direct space-to-time pulse shaper," *Opt. Lett.*, vol. 27, no. 15, pp. 1345–1347, Aug. 2002.

[3] D. Meshulach, D. Yelin, and Y. Silberberg, "Adaptive real-time femtosecond pulse shaping," *J. Opt. Soc. Amer. B, Opt. Phys.*, vol. 15, no. 5, pp. 1615–1619, May 1998.

[4] J. Chou, Y. Han, and B. Jalali, "Adaptive RF-photonic arbitrary waveform generator," *IEEE Photon. Technol. Lett.*, vol. 15, no. 4, pp. 581–583, Apr. 2003.

[5] J. Azana, N. K. Berger, B. Levit, V. Smulakovsky, and B. Fischer, "Frequency shifting of microwave signals by use of a general temporal self-imaging (Talbot) effect in optical fibers," *Opt. Lett.*, vol. 29, no. 24, pp. 2849–2851, Dec. 2004.

[6] J. Azana and L. R. Chen, "General temporal self-imaging phenomena," *J. Opt. Soc. Amer. B, Opt. Phys.*, vol. 20, no. 7, pp. 1447–1458, Jul. 2003.

[7] J. Azana, N. K. Berger, B. Levit, and B. Fischer, "Broadband arbitrary waveform generation based on microwave frequency upshifting in optical fibers," *J. Lightw. Technol.*, vol. 24, no. 7, pp. 2663–2675, Jul. 2006.

[8] J. P. Heritage and A. M. Weiner, "Optical systems and methods based upon temporal stretching, modulation and recompression of ultrashort pulses," U.S. Patent 4 928 316, May 22, 1990.

[9] R. E. Saperstein, N. Alic, D. Panasenko, R. Rokitski, and Y. Fainman, "Time-domain waveform processing by chromatic dispersion for temporal shaping of optical pulses," *J. Opt. Soc. Amer. B, Opt. Phys.*, vol. 22, no. 11, pp. 2427–2436, Nov. 2005.

[10] R. E. Saperstein, D. Panasenko, and Y. Fainman, "Demonstration of a microwave spectrum analyzer based on time-domain processing in fiber," *Opt. Lett.*, vol. 29, no. 5, pp. 501–503, Mar. 2004.

[11] J. Azana, N. K. Berger, B. Levit, and B. Fischer, "Reconfigurable generation of high-repetition-rate optical pulse sequences based on time domain phase-only filtering," *Opt. Lett.*, vol. 30, no. 23, pp. 3228–3230, Dec. 2005.

[12] H. Chi and J. Yao, "Symmetrical waveform generation based on temporal pulse shaping using an amplitude-only modulator," *Electron. Lett.*, vol. 43, no. 7, pp. 415–417, Mar. 2007.

[13] M. A. Muriel, J. Azana, and A. Carballar, "Real-time Fourier transformer based on fiber grating," *Opt. Lett.*, vol. 24, no. 1, pp. 1–3, Jan. 1999.

[14] J. Azana and M. A. Muriel, "Real-time optical spectrum analysis based on the time-space duality in chirped fiber gratings," *IEEE J. Quantum Electron.*, vol. 36, no. 5, pp. 517–526, May 2000.

[15] J. Azana, "Design specifications of a time-domain spectral shaping optical system based on dispersion and temporal modulation," *Electron. Lett.*, vol. 39, no. 21, pp. 1530–1532, Oct. 2003.

[16] M. Miyagi and S. Nishida, "Pulse spreading in a single-mode fiber due to second-order dispersion," *Appl. Opt.*, vol. 18, no. 5, pp. 678–682, Mar. 1979.

[17] M. Amemiya, "Pulse broadening due to higher order dispersion and its transmission limit," *J. Lightw. Technol.*, vol. 20, no. 4, pp. 591–597, Apr. 2002.

[18] T. Komukai and M. Nakazawa, "Fabrication of nonlinearly chirped fiber Bragg gratings for higher-order dispersion compensation," *Opt. Commun.*, vol. 154, no. 1, pp. 5–8, Aug. 1998.

[19] T. Yamamoto and M. Nakazawa, "Third- and fourth-order active dispersion compensation with a phase modulator in a terabit-per-second optical time-division multiplexed transmission," *Opt. Lett.*, vol. 26, no. 9, pp. 647–649, May 2001.

[20] M. D. Pelusi, Y. Matsui, and A. Suzuki, "Electrooptic phase modulation of stretched 250-fs pulses for suppression of third-order fiber dispersion in transmission," *IEEE Photon. Technol. Lett.*, vol. 11, no. 11, pp. 1461–1463, Nov. 1999.

[21] M. Hacker, G. Stobrawa, and T. Feurer, "Iterative Fourier transform algorithm for phase-only pulse shaping," *Opt. Express*, vol. 9, no. 4, pp. 191–199, Aug. 2001.

[22] S. Cialdi, I. Boscolo, and A. Flacco, "Features of a phase-only shaper set for a long rectangular pulse," *J. Opt. Soc. Amer. B, Opt. Phys.*, vol. 21, no. 9, pp. 1693–1698, Sep. 2004.

**Jianping Yao** (M'99–SM'01) received the Ph.D. degree in electrical engineering from the Université de Toulon, Toulon, France, in 1997.

From 1999 to 2001, he held a faculty position with the School of Electrical and Electronic Engineering, Nanyang Technological University, Singapore. Since 2001, he has been with the School of Information Technology and Engineering, University of Ottawa, Ottawa, ON, Canada, where he is currently a Professor, the Director of the Microwave Photonics Research Laboratory, and the Director of the Ottawa–Carleton Institute for Electrical and Computer Engineering. He holds a Guest Professorship with Shantou University, Shantou, China, and Sichuan University, Chengdu, China. He spent three months as an Invited Professor with the Institut National Polytechnique de Grenoble, Grenoble, France, in 2005. His research has focused on microwave photonics, which includes all-optical microwave signal processing, photonic generation of microwaves, millimeter wave and terahertz, radio over fiber, UWB over fiber, fiber Bragg gratings for microwave photonics applications, and optically controlled phased array antennas. His research interests also include fiber lasers, fiber-optic sensors, and biophotonics. He has published over 160 papers in refereed journals and conference proceedings.

Dr. Yao is a Registered Professional Engineer in Ontario. He is a member of SPIE and OSA and a Senior Member of the IEEE LEOS and MTT Societies.

**Hao Chi** received the Ph.D. degree in electronic engineering from Zhejiang University, Hangzhou, China, in 2001.

Since 2003, he has been with the Department of Information and Electronic Engineering, Zhejiang University. Before that, he spent half a year with the Hong Kong Polytechnic University, Kowloon, Hong Kong, as a Research Assistant and two years with Shanghai Jiaotong University, Shanghai, China, as a Postdoctoral Fellow. Since July 2006, he has been with the Microwave Photonics Research Laboratory, School of Information Technology and Engineering, University of Ottawa, Ottawa, ON, Canada. His research interests include optical communications and networking, microwave photonics, fiber-optic sensors, optical signal processing, and fiber grating-based components.